Civil Engineering Infrastructures Journal xx,xx
DOI: 10.22059/CEIJ.2023.362216.1940

Hyperelastic Models for PET Woven Geotextiles in Civil Engineering: Framework and Insights

Author 1:
Fatma Zohra Belhadj1,2*
1*Built Env. Research Lab, Faculty of Civil Engineering, University of Science and Technology, Houari Boumediene (USTHB), Bab Ezzouar, 16311, Algiers, Algeria.
2 Ecole Nationale Superieure des Travaux Publics (ENSTP), 16051, Algiers, Algeria.
Author 2:
Ahmed Fouad Belhadj
3Department of Civil Engineering, University Ferhat Abbas (UFAS), 19000, Setif, Algeria.
Author 3:
Chabaat Mohamed 1
1Built Env. Research Lab, Faculty of Civil Engineering, University of Science and Technology, Houari Boumediene (USTHB), Bab Ezzouar, 16311, Algiers, Algeria.

/ Not Edited

Received: 13/07/2023
Revised: 14/09/2023
Accepted: 16/10/2023

ABSTRACT: The material properties of geotextiles play a significant role in shaping the long-term behavior of reinforced soils, potentially leading to issues like instability and excessive deformation. To address these challenges, thorough research into geotextile materials' rheological properties and nonlinear behavior is essential. This study specifically focuses on the investigation of six commonly employed isotropic hyperelastic models (Neo-Hooke, Mooney-Rivlin, Ogden, Yeoh, Arruda-Boyce, and Van der Waals) for describing the behavior of PET woven geotextiles in civil engineering applications. These models are fine-tuned through uniaxial tension tests conducted in warp and weft directions. Upon analyzing the experimental data, it becomes evident that the Yeoh and Neo-Hooke models exhibit exceptional accuracy in predicting geotextile behavior. The primary objective of this study is to advance our comprehension of how geotextiles react to varying loads, achieved through a combination of testing and finite element simulations. The robust correlation between experimental and simulation results significantly contributes to developing dependable hyperelastic material models tailored for geotextiles. This research framework holds considerable potential value for manufacturers and engineers as it equips them with practical tools to address concerns associated with soil-structure interaction in their projects.

Keywords: Soil-Structure Interaction Interface, Hyperelastic Models, Uniaxial Tension Testing, FEA Modeling.

1. Introduction

In civil engineering, geotextiles find extensive applications, such as soil stabilization, drainage systems, and erosion control. PET woven geotextiles are frequently utilized among various geotextile materials. To comprehensively assess and forecast the performance of PET woven geotextiles under varying loads and environmental conditions, the utilization of hyperelastic models proves beneficial. These models offer a structured approach for gaining

insights into the material's mechanical properties and behavior when deformation occurs.

Hyperelastic models are employed to characterize the stress-strain response of materials that undergo substantially elastic deformations, as is the case with PET-woven geotextiles. These models rely on strain energy density functions, which establish a connection between the energy stored within the material and the deformations it experiences. By selecting an appropriate strain energy density function, it becomes possible to depict the mechanical behavior of the material accurately. Geotextiles and geosynthetics, polymers extensively utilized in civil engineering, geotechnical engineering, and transportation, augment lateral resistance and enhance the properties of backfill materials in foundation systems (Wu et al.,2020).

Ongoing research is directed toward integrating geotextiles into the design process and scrutinizing the interfaces between geotextiles and geomembranes. Researchers employ diverse techniques, including shear tests to assess frictional behavior, triaxial compression tests, and advanced constitutive models such as the one proposed by Guo et al. (Guo et al.,2022). These methodologies yield valuable insights into geotextile-geomembrane interfaces' performance, stability, and mechanical characteristics under varying loading conditions. Cutting-edge constitutive models consider material properties, stress-strain relationships, and interface properties, enabling precise simulation of geotextile behavior and its interaction with geomembranes.

Finite element modeling employs physical tests and a hyperelastic methodology to assess the puncture resistance of needle-punched nonwoven geotextiles (Saberi et al.,2017). This approach scrutinizes these geotextiles' structural integrity and durability by examining their response to puncture loads, thereby facilitating performance prediction and design optimization.

In a broader context, research within civil and geotechnical engineering is primarily centered around analyzing geotextile-geomembrane interfaces and gaining insights into the behavior of geotextiles within foundation systems. Various techniques, including shear tests, triaxial compression tests, constitutive models, and finite element modeling, collectively advance geotextile design and application, ultimately enhancing efficiency and durability in construction projects.

Various constitutive models have been studied, including quasi-linear, hyperbolic, and creep elastoplastic models (Zohra et al.,2022). For simulating reinforced soil, the point material method has been employed, considering fiber interaction through the equivalent additional stress method. Using the estimated rheological viscoelastic behavior presented by Sawicki et al. (Sawicki et al.,1998), some researchers have treated reinforcement as an interface. This involved conducting creep tests on woven and nonwoven geotextiles.

To address the phenomenon of creep as the load increases gradually during partial discharge, the Linear Solid Model (LSM) has been developed. Additionally, two modified viscoelastic models have been explored to account for plastic deformations in geotextiles. Ding et al. (Ding et al.,2023) proposed a constitutive model that captures the creep behavior and stress relaxation of geogrids under various loading levels.

wang et al. (Wang et al.,2020) investigated the creep deformation and stress relaxation of polymer geosynthetics using conventional test methods. Jeon et al. (Jeon et al.,2009) examined the stress relaxation behavior of geosynthetics under additional stresses and/or elevated temperatures. Lastly, Peng et al. (Peng2010 et al.,) introduced an elasto-viscoplastic constitutive model to simulate the velocity-dependent behavior of polymeric geosynthetics.

2. Material and Methods

Phenomenological and micromechanical models use extensively in characterizing the elastic and nearly incompressible mechanical responses of materials that undergo deformation under low loads and retain their deformations even after the load removal. In polymers and plastics, a common approach involves employing non-Gaussian force-extension relationships (Treloar ,1975), which are tailored to stress-strain data obtained from uniaxial tests (Hackett ,2016). These relationships are instrumental in capturing hyperelasticity curves, along with their corresponding parameters, as well as describing isotropic elastic properties.

However, it's important to note that distinct hyperelastic material systems necessitate specific properties for characterizing Cauchy-Green tensor

Accepted / Not Edited

strains, central strain ratios, stretching behavior, and simulation stress energies (Mansouri et al.,2014).

Hyperelastic constitutive models, such as the Mooney-Rivlin and Ogden models, find widespread use in the characterization and design of the viscoelastic behavior of various materials under conditions involving finite strains (Heymans et al.,2004l). These materials encompass synthetic polymers, vulcanized rubber, and biological substances.

While the Mooney-Rivlin and Ogden models serve as standard choices for isotropic hyperelastic modeling (Kang et al.,2018), other models like the Ogden-Yeoh and Arruda Boyce models have been extensively tested and applied to specific materials like rubber and flexible foams (Kenja et al.,2020, li et al.,2016).

The calibration of these models for soft and surrogate tissues considers experimental factors that influence uniaxial test data. As a result, this work delves into exploring a range of hyperelastic material models, both phenomenological and micromechanical, intending to describe the mechanical behavior of PET woven geotextiles accurately. This investigation takes into account the viscoelastic properties and finite-strain conditions characteristic of these materials.

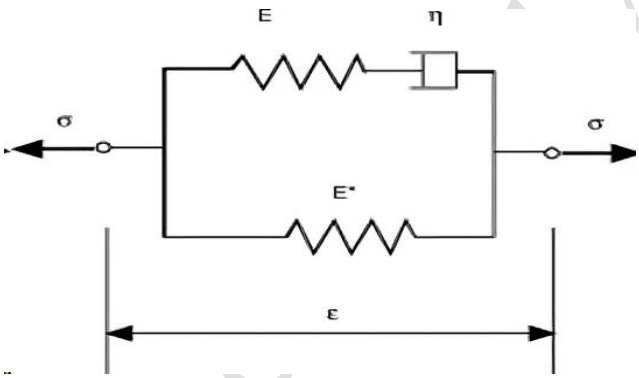

Fig. 1. Rheological coefficients of the Zener model (chevalier2001modification)

The Mooney-Rivlin model (Mihai et al.,2017) utilizes a strain energy density function resembling the Neo-Hookean model and is frequently employed in characterizing material behavior. However, in cases involving rubber materials or flexible foams with restricted elasticity, alternative models like Ogden-Yeoh, Arruda Boyce, and Blatz have undergone thorough testing and are commonly utilized.

In a study conducted by Narayanan et al. (Narayanan et al.,2023), a range of hyperelastic constitutive models, including polynomial, Ogden, Arruda-Boyce, and Van der Waals forms, were investigated for their suitability in finite element analysis (FEA) of large elastic deformations in isotropic materials. These materials encompassed incompressible and nearly incompressible substances, such as elastomers and PET polymers used in geotextiles.

Notably, the Ogden (Yun et al.,2021), Arruda-Boyce (Mokhireva et al.,2020), and Van der Waals models were found to exhibit viscoelastic behavior (Brinson et al.,2008). The study demonstrated that even relatively simple constitutive models, readily available in FEA software, yielded promising results for nearly incompressible materials.

This comparative analysis examines various hyperelastic constitutive models for their applicability in characterizing the mechanical behavior of PET woven geotextiles. The results provide valuable insights into selecting suitable models for accurately representing the viscoelastic properties and accommodating large elastic deformations in these materials.

The optimization technique known as the Levenberg-Marquardt algorithm is used to calibrate the hyperelastic material models. This technique is widely recognized for minimizing errors between model predictions and experimental data. It is a nonlinear least squares optimization algorithm often used to calibrate hyperelastic material models (Gavin et al.,2019, Van et al.,2020) based on the Gauss-Newton algorithm. The Gauss-Newton method is a linearization method that assumes the model is linear around the current parameter estimates. This assumption is often violated in nonlinear problems, leading to convergence problems. The Marquardt method introduces a regularization term into the objective function that penalizes significant changes in the parameter estimates. This helps improve the algorithm's robustness to ill-conditioning and can help prevent it from getting stuck in local minima.

The Levenberg-Marquardt algorithm is a powerful and versatile optimization algorithm that can be used to calibrate a wide variety of models. It is particularly well-suited for calibrating hyperelastic material

Accepted / Not Edited

models because it is robust to ill-conditioning and can converge quickly.

2.1 Insights into Stress-Strain Relationships for Hyperelastic Models

This study focuses on geotextile samples comprising synthetic fibers, notably polyethylene terephthalate (PET) (Chevalier et al.,2012). Polyester, the material employed to produce these fibers, is a composite of ethylene glycol and terephthalic acid (or dimethyl terephthalate) (Carreau et al.,2021). Polyester is selected for geotextiles owing to its advantageous characteristics, including a high modulus, resistance to creep, and chemical inertness. The scope of this study is primarily limited to hyperelastic constitutive models that establish the relationship between strain and stress based on material properties. The strain energy function (W) is a crucial aspect of these models and is differentiated for each invariant of the Cauchy-Green deformation tensor. It can be expanded in an infinite power series of the Cauchy-Green deformation tensor. Under the condition of incompressibility, the strain energy function can be expressed as:

$$w = f(I_1 \ I_2 \ I_3) \quad (1)$$

Where w is the strain energy potential, $I_1 \ I_2 \ I_3$ are the invariants of the Cauchy-Green deformation tensors.

Through our examination of these hyperelastic constitutive models, our objective is to attain a more profound comprehension of the mechanical characteristics exhibited by PET geotextiles and how they react under diverse loading conditions. The strain energy function for hyperelastic constitutive models is expressed in Equation 1. The material properties are determined based on the invariants of the I1, I2, and I3. These invariants are mathematically defined in terms of the principal stretches, λ1, λ2, and λ3, derived from the deformation tensor. Hyperelastic constitutive models are highly effective in accurately describing material behavior during significant deformations. They achieve this by utilizing the strain energy function and the derivation of material parameters from the Cauchy-Green deformation tensors. A comprehensive understanding of this interplay is essential for accurately predicting and analyzing material responses in various engineering applications.

In the scenario of uniaxial tension applied to an incompressible material, where σ2 = σ3 = 0, the invariants can be conveniently expressed in terms of the stretch along the direction of tension, λ1, as demonstrated in Equation 5. To compute both the strain, ε, and the stretches, λi, specifically for this situation, one can effectively utilize Equations 6 and 7, respectively. These equations employ the initial length of the sample as a reference point for the calculations.

$$I_1 = \lambda_1^2 + \lambda_2^2 + \lambda_3^2 \quad (2)$$

$$I_2 = \lambda_1^2 \lambda_2^2 + \lambda_2^2 \lambda_3^2 + \lambda_3^2 \lambda_1^2 \quad (3)$$

$$I_3 = \lambda_1^2 \lambda_2^2 \lambda_3^2 \quad (4)$$

$$\lambda_1^2 \lambda_2^2 \lambda_3^2 = 1 \quad (5)$$

Where $\lambda_1 \ \lambda_2 \ and \ \lambda_3$ are the principal stretches,derived from the deformation tensor $I_1 \ I_2$ and I_3. We can establish a clear relationship between the applied uniaxial tension, the resulting strain, and the stretches in various directions using these equations. This knowledge holds significant importance in comprehending how materials behave under uniaxial tension and is pivotal for making accurate predictions regarding material responses in engineering applications.

$$\varepsilon = \frac{\Delta l}{l_0} \quad (6)$$

$$\lambda = \varepsilon + 1 \quad (7)$$

Where ε is the stain ratio, l_0 is the inial lenth and Δl is the leth variation. The following are some of the hyperelastic constitutive models that are commonly used to describe the mechanical behavior of materials:

Reduced polynomial model: This model is a simplified version of the Ogden model that uses a polynomial function of the first invariant of the Cauchy-Green tensor. It is a good choice for materials that exhibit a linear relationship between stress and strain.

Mooney-Rivlin model: This is a two-parameter model that uses the first and second invariants of the Cauchy-Green tensor to describe the strain energy

Accepted / Not Edited

function. It is a good choice for materials that exhibit nonlinear elastic behavior.

Neo-Hookean model: This one-parameter model uses the second invariant of the Cauchy-Green tensor to describe the strain energy function. It is a good choice for materials that exhibit small elastic deformations.

Yeoh model: This three-parameter model uses the first invariant of the Cauchy-Green tensor to describe the strain energy function. It is a good choice for materials that exhibit nonlinear elastic behavior and are incompressible.

Arruda-Boyce model: This four-parameter model uses the first invariant of the Cauchy-Green tensor to describe the strain energy function. It is a good choice for materials that exhibit nonlinear elastic behavior and are compressible.

2.2 Reduced Polynomial Model

Initially introduced by Rivlin, the reduced polynomial model has been expanded to encompass N values up to 6, significantly enhancing its capacity to capture intricate strain behaviors. At N=3, this model aligns with the Yeoh model, and at N=1, it corresponds to the Neo-Hookean model. The reduced polynomial model primarily leverages the first invariance (I1) and demonstrates minimal sensitivity to variations in stress-energy encompassed within the second invariance (I2). This distinctive characteristic renders it an attractive choice for predicting complex strain behaviors, even in scenarios with limited experimental data. The shear modulus of the reduced polynomial model is explicitly defined as μ0 = 2C10, and its energy potential is expressed by Equation 8. Researchers and engineers can harness this model effectively to anticipate and analyze material strain responses, providing valuable insights for various engineering applications.

$$W = \sum_{i=1}^{N} C_{10}(I_1 - 3)^i \sum_{i=1}^{N} \frac{1}{D_i}(j_{el} - 1)^{2i} \quad (8)$$

Where $\boldsymbol{W}$ is strain energy potential, $\boldsymbol{j_{el}}$ the elastic volume ratio, $\boldsymbol{C_{10}}$ is material shear behavior constant and $\boldsymbol{D_i}$ is constant for incomprsessible metrials.

2.3 The Mooney-Rivlin Model

Prior research has convincingly demonstrated the efficacy of the Mooney-Rivlin model, an elastic model, in accurately characterizing moderate to large strains and shear deformations occurring in uniformly dilated or contracted planes (Mooney ,1940, Rivlin ,1948). This model finds widespread use for representing the elasticity of gels and tissues. The strain-energy function for the Mooney-Rivlin model has been derived in a general form (Barbero ,2023), with its specific expression provided in Equation 9. The Mooney-Rivlin model is pivotal in faithfully modeling the mechanical behavior of materials undergoing significant strains and shear deformations. Its formulation yields valuable insights for comprehending and forecasting the behavior of diverse materials, especially in contexts involving gels and tissues.

$$W = C_{10}\,(I_1 - 3)\,C_{01}(I_2 - 3)\,\frac{1}{D_i}(j_{el} - 1)^2 \quad (9)$$
$$C_{10} = \frac{\mu_1}{2} \quad and\ C_{01} = -\mu_2$$

Where $C_{01,} and\ C_{10}$ are material constants or parameters repectively, define the behavior of the material being modeled. μ_1 μ_2 are constants related to the material's viscoelastic properties .

2.4 Neo-Hooke model

The Neo-Hooke, an elastic model that employs a nonlinear approach grounded in Hooke's law, excels at handling relatively modest deformations effectively. However, it is limited because it cannot account for stress recovery. In scenarios where material data is unavailable, the model can be simplified by setting C01 to 0, resulting in a widely used subset of the Mooney-Rivlin model (Shahzad et al.,2015). While the Neo-Hooke model is user-friendly and performs admirably for small deformations, it cannot account for stress and strain recovery. The mathematical representation for the strain-energy function employed in the Neo-Hooke model is provided in Equation 10. This model imparts valuable insights into the mechanical behavior of materials subjected to small deformations. Still, its inability to capture stress recovery must be considered when applying it to engineering analyses.

Accepted / Not Edited

$$W = C_{10}\,(I_2 - 3)\frac{1}{D_1}(j_{el} - 1)^{\,2} \qquad (10)$$

The Yeoh model presents a mathematical approach employing a third-order polynomial equation grounded in the first invariant of the strain tensor. It is adept at accurately characterizing the nonlinear elastic behavior of materials like rubber and plastic when subjected to significant deformations. This model can fit experimental data and capture a broad spectrum of deformation patterns, demanding only minimal input information. Furthermore, the reduced polynomial variant of the Yeoh model is suitable for compressible materials. It yields precise forecasts of the stress-strain response for various substances, including carbon-filled black rubber. The strain-energy function utilized in the Yeoh model is expressed mathematically through Equation 10.

By employing the Yeoh model, researchers and engineers can proficiently analyze and predict the nonlinear elastic behavior of materials, delivering invaluable insights applicable across a wide array of applications.

$$W = \sum_{i=1}^{3} C_{i0}(I_1 - 3)^i \sum_{i=1}^{3} \frac{1}{D_i}(j_{el} - 1)^{2i} \qquad (11)$$

2.5 Arruda-Boyce Model

A third-order polynomial model, relying on the first invariant of the strain tensor, finds extensive use in characterizing the nonlinear elastic behavior of materials such as rubber and plastics when subjected to significant deformations (Arruda et al.,1993). This versatile model fits experimental data and effectively describes a wide range of deformation patterns. Moreover, the reduced polynomial variant of this model is especially well-suited for compressible materials, offering precise forecasts of the stress-strain response across diverse materials, including carbon-filled black rubber. Mathematically, the strain-energy function employed in this model can be expressed as follows:

$$W = \mu \sum_{i=1}^{5} \frac{C_i}{\lambda_m^{2i-2}}\left(I_1^i - 3^i\right)\frac{1}{D}\left\{\frac{j_{el}^2 - 1}{2} - ln\, j_{el}\right\} \qquad (12)$$

$C_1 = \frac{1}{2}$, $C_2 = \frac{1}{20}$, $C_3 = \frac{11}{1050}$, $C_4 = \frac{19}{7000}$
$C_5 = \frac{519}{673750}$

$$\mathrm{D} = \frac{9K + 8\mu}{3(K + 2\mu)}$$

Where, λ_m is the initial shear modulus and the locking stretch, which refers to the point where the stress-strain curve experiences a notable increase in the upturn. K denote the initial bulk modulus, and D is double the inverse initial bulk modulusn,while μ represents the initial shear modulus. Using this third-order polynomial model, researchers and engineers can proficiently analyze and predict the nonlinear elastic behavior of materials, facilitating a deeper understanding and enabling practical applications across numerous fields.

2.6 Van Der Waals Model

The Van der Waals model, also known as Kilian's model, is a hyperelastic potential extensively employed for describing the nonlinear elastic behavior of materials (Mihai et al.,2017). This comprehensive model encompasses equations for various parameters, including primary stretches, the Jacobean determinant, the locking stretch λm, and the linear mixture parameter β. The strain energy function of the Van der Waals model, as outlined in Equation 13, relies on the initial shear modulus μ and the inverse initial bulk modulus D. Additionally, the model incorporates three parameters: I, η, and α, which are defined by equations 14, 15, and 16, respectively.

$$\mathrm{w} = \mu\left\{-\left(\lambda_m^2 - 3\ln[(1-\eta) + \eta] - \frac{2\alpha}{3}\right)\left(\frac{\tilde{I} - 3}{2}\right)^{3/2} + \frac{1}{D}\left[\frac{j_{el}^2 - 1}{2} - ln(j_{el})\right]\right\} \qquad (13)$$

$$\tilde{I} = (1 - \beta)I_1 + I_2\beta \qquad (14)$$

$$\eta = \sqrt{\frac{I - 3}{\lambda_m^2 - 3}} \qquad (15)$$

$$\alpha = \frac{2C_{01}}{3\mu} + \frac{\lambda_m^2}{\lambda_m^3 - 1} \qquad (16)$$

Accepted / Not Edited

Where, β, η and α are intermediate variables and measures related to the material's deformation within the Van der Waals hyperelastic model, aiding in the calculation of the strain energy function and providing insights into the material's behavior under deformation. The Van der Waals model facilitates precise analysis and characterization of the nonlinear elastic behavior of materials. Its incorporation of multiple parameters yields valuable insights applicable across various engineering applications.

2.7 Ogden Model

The Ogden model, introduced by Ogden (Yun et al.,2021), is a mechanical model that describes the elasticity of materials experiencing non-uniform deformation. It utilizes a strain energy function that integrates material parameters and strain invariants. Diverging from constant-based models, the Ogden model's dependency on the principal strain sets it apart. Equation 17 depicts the mathematical representation of the strain energy function (Lim et al.,2011).

$$W=\sum_{i=1}^{n}\frac{2\mu_1}{\alpha_i^2}\left(\bar{\lambda}_1^{\alpha_1}+\bar{\lambda}_2^{\alpha_1}+\bar{\lambda}_3^{\alpha_1}-3\right)\sum_{i=1}^{N}\frac{1}{D_i}(j_{el}-1)^{2i} \quad (17)$$

The reduced polynomial model is a simplified version of the Ogden model that is easier to implement and can be used to model a broader range of materials. The Mooney-Rivlin model is a two-parameter model often used to model rubber-like materials. The Neo-Hookean model is a one-parameter model often used to model materials exhibiting small elastic deformations. The Yeoh model is a three-parameter model that is often used to model materials that exhibit nonlinear elastic behavior and are incompressible. The Arruda-Boyce model is a four-parameter model often used to model materials that exhibit nonlinear elastic behavior and are compressible.

The choice of which model to use depends on the modeled material and the accuracy required. The reduced polynomial model is the simplest option, but it may need to be more accurate for some applications. The Mooney-Rivlin model is a good compromise between accuracy and simplicity. The Neo-Hookean model is the simplest one that can accurately capture the behavior of materials exhibiting small elastic deformations. The Yeoh model is a good choice for materials that exhibit nonlinear elastic behavior and are incompressible. The Arruda-Boyce model is a good choice for materials that exhibit nonlinear elastic behavior and are compressible.

3. Characterizing Geotextile Materials through Uniaxial Tension Testing

This section is dedicated to the characterization of geotextile materials through uniaxial stress testing. In this testing method, the material undergoes tension in one direction while the other remains constant. This enables the measurement of the material's reaction to deformation along a single axis, offering valuable insights into its mechanical behavior. The mechanical setup, as shown in Figure 2, features a PET-woven geotextile sample and a traction machine equipped with geotextile strips.

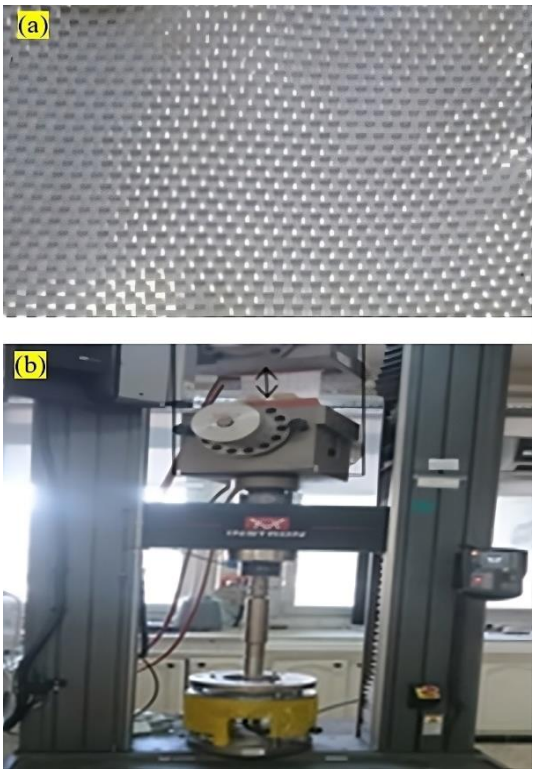

Fig. 2. (a) Test specimen (PET woven geotextile), (b) Traction machine with geotextile strips

Accepted / Not Edited

$$E_I = \frac{\partial \sigma^e}{\partial \varepsilon^e} \quad (18)$$

$$E_{II} = \frac{\partial \sigma^{en}}{\partial \varepsilon^{en}} \quad (19)$$

Tension tests were performed on dumbbell-shaped PET specimens (Treloar ,1943, Treloar1979) with a minimum aspect ratio of 2.5 and a length of 50mm (Iso ,2008) (refer to Figure 2). These tests were carried out using a constant-speed testing machine, and the resultant tensile strength-extension curves were scrutinized to extract the material's stiffness parameters and tensile strength. The curves display nonlinear behavior, underscoring the inapplicability of Hooke's law and emphasizing that the modulus of elasticity can only be valid within a restricted strain range.

The material was clamped between two sheet metal sheets bonded to form a standard tension rod for conducting the uniaxial tension tests. This rod was subsequently affixed to a tensile testing machine for assessment. To measure strain, the thinnest portion of the rod was chosen, and drilled plates were affixed to determine strength and tensile strength. It's worth noting that the modulus of elasticity varies depending on the levels of both linear and nonlinear elastic strain (Lagan et al.,2007).

- **Phase I,** often called the "toe region," is distinguishable by a low modulus of elasticity and significant deformation. This behavior arises from the presence of elastin fibers in the skin, which are pivotal in facilitating stretching mechanisms (E_I).
- **Phase II,** alternatively termed the "linear region," is marked by an escalation in stiffness. This shift occurs as the fibers within the skin progressively align and straighten (E_{II}).

Where E_I and E_{II} represent the elastic modulus related to phase I and phase II, respectively.
The resultant mechanical properties of the material, encompassing the elastic modulus (E_I and E_II)

computed using Equations 18 and 19, along with the maximum tensile strength for both the warp and weft test directions, are briefly presented in Table 1. The tests were conducted using a constant-speed testing machine.

Subsequently, the resulting tensile strength-extension curves underwent analysis to ascertain the material's stiffness parameters and tensile strength. It was observed that these curves displayed nonlinear behavior, signifying the inapplicability of Hooke's law and the limited range for which the modulus of elasticity can be employed. The stress-strain curve from the tension test can be categorized into linear elastic and nonlinear plastic regions, as illustrated in Figure 3. The mechanical properties of the material, derived by plotting sample strength against stretch, are briefly summarized in Table 1.

Accepted / Not Edited

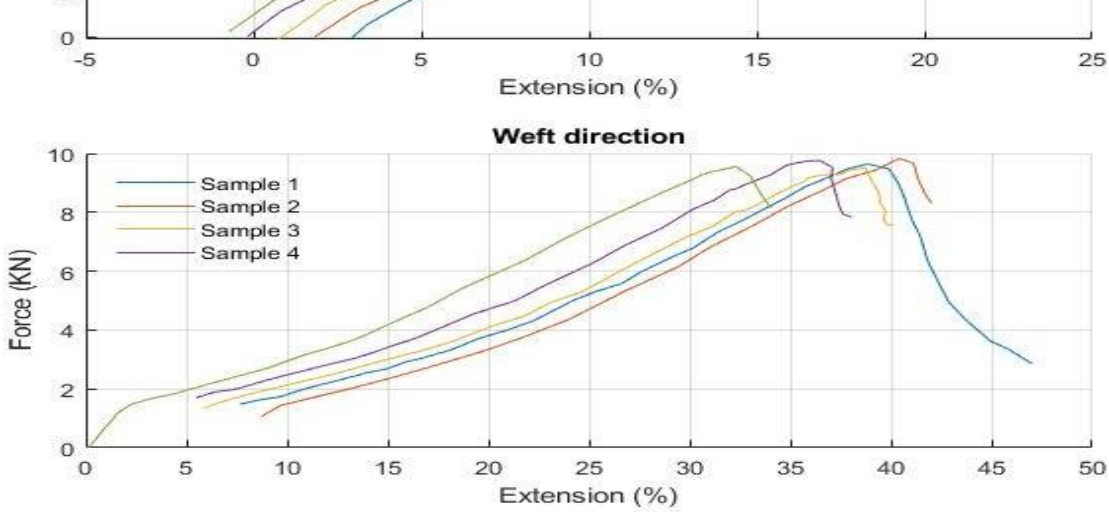

Fig. 3. Stretch test experiments in two orientations with four samples

Table 1. Geotextile material properties

Material Model	Coefficients	Sample 01	Sample 02	Sample 03	Sample 04
Weft Test direction	Elastic modulus EI [MPa]	691.07	652.10	613.63	521.64
	Elastic modulus EII [MPa]	193.22	203.15	191.60	191.60
	Max Tensil stenght (KN/m)	149.26	150.28	151.25	152.33
Warp Test direction	Elastic modulus EI [MPa]	2,343.58	1,827.31	2,559.77	2,043.58
	Elastic modulus EII [MPa]	1,903.19	1,833.55	1,673.27	1,624.03
	Max force/wide KN/m	47.94	49.12	48.12	47.94

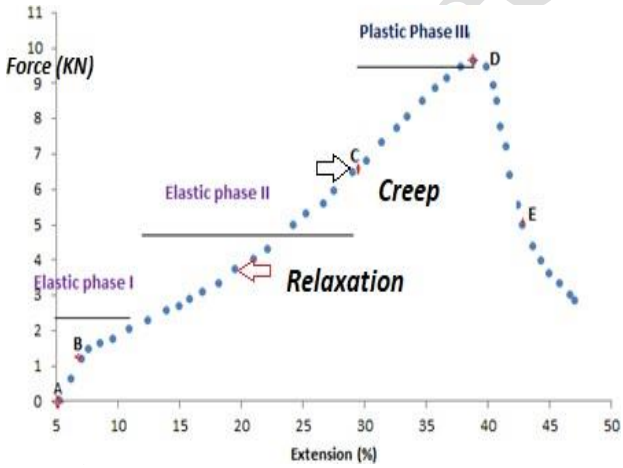

Fig. 4. Load extension segmented curves related to sample in the weft direction

According to (Ward et al.,2012), Hooke's stress-strain relation represents a linear constitutive relation applicable to ideal elastic, isotropic solids under low strains. This law establishes that stress is directly proportional to strain, with the modulus of elasticity or Young's modulus as the constant of proportionality. However, when grappling with high strains, it becomes essential to employ nonlinear constitutive relationships, as discussed in (Hackett2016), to precisely depict the mechanical characteristics of materials. Table 1 offers an overview of the laboratory properties of geotextiles, encompassing both their elastic and nonlinear behavior when subjected to uniaxial deformation.

3.1 PET Geotextile Samples Per Direction

During the stretching process, the specimens experience irreversible plastic deformation, which progressively increases as the deformation continues. When the strain is below the yield strength, the stress resulting from plastic strain remains relatively constant. The material undergoes stiffening and displays nonlinear behavior due to the

Not Edited

increased rigidity of the molecular chains. The maximum elongation, approximately 40%, corresponds to a stress of nearly 150 KN/m in the weft direction, whereas it is only 50 KN/m in the warp direction, as indicated in the manufacturer's technical data sheet. The following are the key points noted from Table 1.

- The elastic modulus EI is higher in the warp direction than the EII in the warp and weft test directions. This suggests that the material exhibits greater stiffness in the warp direction than in the weft direction.
- The maximum tensile strength is also notably higher in the warp direction than in the weft direction.
- The material displays nonlinear behavior, as evidenced by the curves in Figure 4. This implies that Hooke's law does not apply to this material, and the modulus of elasticity can only be used ithin a limited strain range.

Constitutive relations are mathematical representations used to describe the mechanical behavior of materials, and they can be categorized into two main types: linear and nonlinear. Hooke's law exemplifies a linear relation, typically applicable to ideal elastic, isotropic solids undergoing low strains. However, employing nonlinear constitutive relations to represent material behavior accurately becomes essential when dealing with high strains. The stress-strain curve, elaborated in references (Powell et al.,2023), illustrates the typical response of polymers, encompassing elastic deformation, yield, plastic flow, necking, strain hardening, and eventual fracture. The diagram presented in (Hieu et al.,2023) summarizes typical behavior as follows. The stress-strain curve exhibits three distinct regions:

- **Region 1**: This initial region is characterized by a linear relationship between stress and strain, known as the elastic region, where the material undergoes reversible deformation.
- **Region 2**: This subsequent region is characterized by a nonlinear relationship between stress and strain, denoted as the plastic region, where the material undergoes irreversible deformation.
- **Region 3:** The final region is characterized by a decrease in stress with increasing strain, known as the necking region, where the material forms a neck and eventually fails.

The stress-strain curve also includes two transitional phases:

- The yield point marks the point where the material initiates plastic deformation.
- The necking point: This signifies the point at which the material begins to form a neck.

Figure 4 illustrates these three distinct regions and the two transitional phases. In the initial region, stress exhibits a linear increase, followed by a more gradual increment as deformation advances (phase II), ultimately resulting in irreversible plastic deformation. Significant morphological changes mark this phase, including material fragmentation and the release of stored elastic energy. Additionally, the diagram denotes two transitional regions.

4. Data Test Calibration

The stress-strain curve of polymers displays three distinct regions and two transition phases: elastic deformation, yield, plastic flow, necking, strain hardening, and fracture. To precisely characterize a material's mechanical behavior, the material calibration process is employed. This entails determining the parameters of a constitutive model by comparing experimental data, such as stress-strain curves, with model predictions and fine-tuning the model parameters until a close match is attained. Optimization techniques, like least squares or maximum likelihood Sample orientation, can influence experimental outcomes and the mathematical coefficients employed in evaluating isotropic hyperelastic constitutive laws. Consequently, variations may arise in the selection of the hyperelastic model and the determination of material constants. This influence can be observed in the strain energy function derived from uniaxial testing, as well as in the resulting coefficients and the root mean square error (R2), which are presented in Tables 2 and 3.

Accepted / Not Edited

Estimation can be applied for parameter refinement. However, the precision of the calibrated model hinges on the quality and quantity of the experimental data used during the calibration process. The tables present the outcomes of calibrating various hyperelastic material models for the geotextile samples' warp and weft directions. These models encompass the Mooney-Rivlin, Ogden, Arruda-Boyce, Neo-Hookean, and Van-der-Waals models. The tables display the coefficients associated with each model, accompanied by R-squared values.

4.1 Material Evaluation for Warp Sample Orientation

It is important to acknowledge that factors such as sample orientation can also impact the assessment of hyperelastic constitutive laws, as detailed earlier in this section. Uniaxial testing was performed on each pair to assess material behavior for the warp sample orientation. The goal was to identify the most precise model for characterizing material behavior and constructing a strain energy function based on invariants or stretches. The test results for the different deformation modes investigated are detailed in Section 2.1 and illustrated in Figure 3. The calibration process for hyperelastic models involves minimizing the error between the predicted stress-strain response of the model and experimental data. The following steps are involved:

- Initialize the model parameters.
- Calculate the predicted stress-strain response of the model.
- Calculate the error between the predicted stress-strain response and the experimental data.
- Repeat steps 2-4 until the error is minimized.

We use a numerical optimization algorithm to calibrate hyperelastic models by minimizing the error between the predicted and experimental stress-strain responses. The stress TU is the nominal or engineering stress. For the case of uniaxial deformation, the relationship between nominal stress and stretch is given by Eq20, regardless of the specific form of the strain energy function. This is because the first invariant of the right Cauchy-Green deformation tensor is the same for all these models.

$$T_U = 2(\lambda - \frac{1}{\lambda})C10 \quad (20)$$

Where, T_U represents the nominal stress

Table 2. Models' calibration for warp direction.

Materiel Model	Coefficients	Sample 01	Sample 02	Sample 03	Sample 04
Mooney-Rivlin D=0	C10(MPa)	1.94	1.76	2.00	1.92
	C1(MPa)	1.39	1.92	-0.87	-1.57
Ogden N=1	μI	4.24	5.54	3.01	2.10
	α with DI = 0	1.97	1.79	2.13	2.28
	R2	29.8	29.5	10.99	24.09
Arruda-Boyce	μ = μ0	4.14	4.23	3.34	2.53
	λm	9197	18579	13	9.15
	R2	29.6	21.18	12.08	25.82
Neo-Hookean	C10(MPa)	2.07	2.11	1.79	1.45
	R2	16.2	15.2	11.2	12.5
Yeoh material	C10(MPa)	2.00	2.40	1.51	1.105
	C20(MPa)	5.54	-5.45	8.28	1.08
	C30(MPa)	-4.19	1.76	-4.46	-5.14
	R2	18.5	14.3	11.6	13.5
Van-Der-Waals	μ	4.36	5.52	3.11	2.17
	λ	1113	27	1036	867.7
	A	1.27	0.122	-3.3	-9.15
	R2	29.5	19.05	11.36	24.41

Accepted / Not Edited

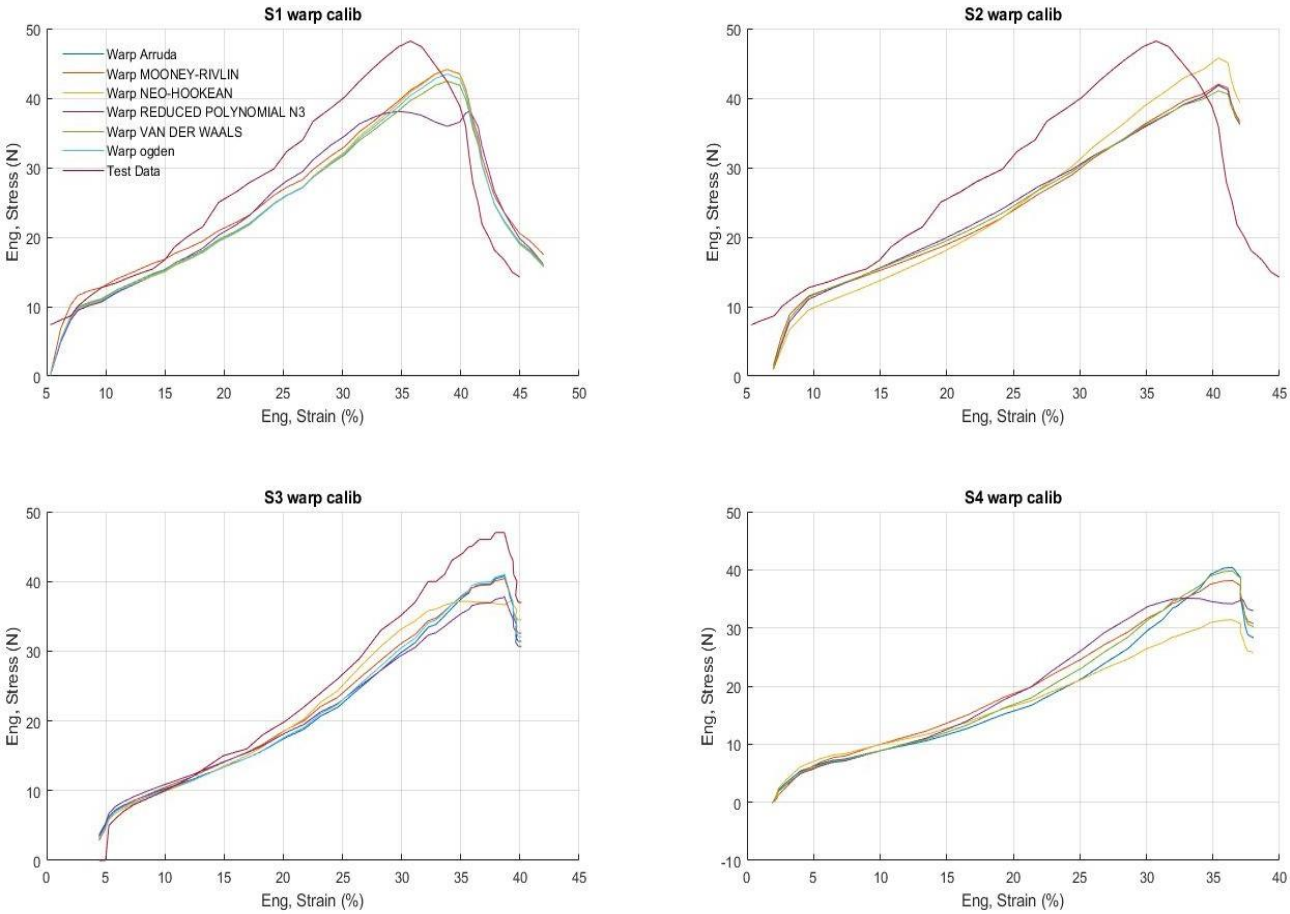

Fig. 5. Fitting hyperelastic models to all sample warp experimental findings

Based on the results presented in Table 2, the Van der Waals, Ogden, Arruda-Boyce, and Neo-Hook hyperelastic material models were identified as more suitable for predicting geotextile behavior than the Mooney-Rivlin and Yeoh models. This selection was based on several key factors and considerations:

- Model Fit (R2 Value): As indicated by the coefficient of determination (R2), the goodness of fit was one of the primary criteria for model selection. Higher R2 values suggest a better fit of the model to the experimental data. Among the models tested, the Van Der Waals, Ogden, Arruda-Boyce, and Neo-Hook models consistently demonstrated higher R2 values than the Mooney-Rivlin and Yeoh models; these models better represented the geotextile behavior under the given conditions.

- Parameter Stability: The stability of the model parameters across different samples is crucial for reliable predictions. The selected models exhibited relatively stable parameter values (coefficients) across the tested samples, indicating their robustness and ability to capture the material behavior consistently.

- Physical Justification: Each of the selected models has a physical basis or theoretical foundation that aligns with the behavior of geotextiles under uniaxial loading. These models are well-established in material modeling and have been successfully applied to various materials, including elastomers and polymers.

- Predictive Accuracy: During the calibration process, the selected models demonstrated a higher degree of accuracy in predicting the mechanical behavior of geotextiles under uniaxial loading conditions. This accuracy is essential for practical engineering applications requiring precise material behavior predictions.

Accepted

- Model Simplicity: While the selected models are sophisticated in their formulation, they do not introduce unnecessary complexity. They balance accuracy and simplicity, making them practical for engineering analysis and design.

In sum, the choice of the Van Der Waals, Ogden, Arruda-Boyce, and Neo-Hook hyperelastic material models was based on their superior fit to the experimental data, stability across samples, physical relevance, predictive accuracy, and practical applicability in the context of geotextile behavior modeling. These models offer a robust framework for characterizing and predicting the mechanical response of geotextiles under uniaxial loading, which is essential for geotechnical engineering applications.

The findings presented in Table 2 show that the Van Der Waals, Ogden, Arruda-Boyce, and Neo-Hook hyperelastic material models have a higher coefficient of determination (R2) than the Mooney-Rivlin and Yeoh models. The coefficient of determination measures how well the model fits the data. A higher R2 value indicates a better fit. In other words, the Van Der Waals, Ogden, Arruda-Boyce, and Neo-Hook models can predict the behavior of geotextiles more accurately than the Mooney-Rivlin and Yeoh models because the Van Der Waals, Ogden, Arruda-Boyce, and Neo-Hook models are more complex and consider more factors that affect the behavior of geotextiles.

The Mooney-Rivlin and Yeoh models are simpler based on the assumption that the strain energy density is a function of the first and second strain invariants. The Van Der Waals, Ogden, Arruda-Boyce, and Neo-Hook models are more complex based on the assumption that the strain energy density is a function of the first, second, and third strain invariants. This latest invariant is a measure of the volume change of the material. Including the third strain invariant in the Van Der Waals, Ogden, Arruda-Boyce, and Neo-Hook models makes them more accurate for predicting the behavior of geotextiles, which are often subjected to significant volume changes.

In addition, the Van Der Waals, Ogden, Arruda-Boyce, and Neo-Hook models can capture geotextiles' nonlinear behavior better than the Mooney-Rivlin and Yeoh models. Geotextiles are often subjected to large deformations, and the nonlinear behavior of these materials becomes more pronounced at large deformations. The Van Der Waals, Ogden, Arruda-Boyce, and Neo-Hook hyperelastic material models are more suitable for predicting geotextile behavior than the Mooney-Rivlin and Yeoh models.

4.1 Material evaluation: Weft Sample Orientation

Table 3 presents the calibration results of various hyperelastic material models for the weft direction of geotextiles. These models include Mooney-Rivlin, Ogden, Arruda-Boyce, Neo-Hookean, Yeoh, and Van-Der-Waals. The table shows the coefficients of these models for different samples (Sample 01, Sample 02, Sample 03, and Sample 04) in terms of their respective material parameters.

The evaluation of the weft sample orientation involved utilizing multiple models, with their results being compared and analyzed. A significant differentiation among these models lies in how they compute strain energy density. While the Mooney-Rivlin model relies on primary strain invariants, the Ogden model considers three primary sections. Consequently, these two models yield distinct outcomes for the weft direction, as illustrated in Figure 6.

The calibration results for the weft direction reveal that the Van Der Waals, Ogden, Arruda-Boyce, and Neo-Hook hyperelastic material models exhibit higher R-squared values than the Mooney-Rivlin and Yeoh models. That signifies that the Van Der Waals, Ogden, Arruda-Boyce, and Neo-Hook models offer a better fit to the experimental data for the weft direction of the geotextile samples. In contrast, the Mooney-Rivlin and Yeoh models display lower R-squared values, indicating a less accurate fit to the data.

The Neo-Hookean model has the highest R-squared value among the three samples; it implies that, for three out of the four samples, the Neo-Hookean model best aligns with the experimental data for the weft direction of the geotextile samples. Other models show lower R-squared values, suggesting they are less suitable for this dataset.

Accepted / Not Edited

Table 3. Calibration of models for weft direction

Material Model	Coefficients	Sample 01	Sample 02	Sample 03	Sample 04
Mooney-Rivlin D=0	C10(MPa)	0.29	0.28	0.31	0.30
	C01(MPa)	0.93	0.57	2.05	2.38
Ogden N=1	μI	1.37	0.92	0.52	0.18
	α with DI = 0	1.72	1.84	2.05	2.38
	R2	12.11	24.89	9.79	10.65
Arruda-Boyce	μ = μ0	0.70	0.64	0.55	0.33
	λm	62946	42139	45	22
	R2	12.11	26.3	9.79	10.65
Neo-Hookean	C10(MPa)	0.35	0.30	0.29	0.20
	R2	18.2	19.12	13.95	14.78
Yeoh material C20=C30	C10(MPa)	0.48	0.38	0.27	0.13
	R2	20.82	26.30	9.67	21.10
Van-Der-Waals	Mu	1.17	0.79	0.72	0.24
	λm	59.03	95.68	1064.7	94.31
	A	6.89	3.27	0.013	-0.04
	R2	12.69	25.12	9.35	14.67

Not Edited

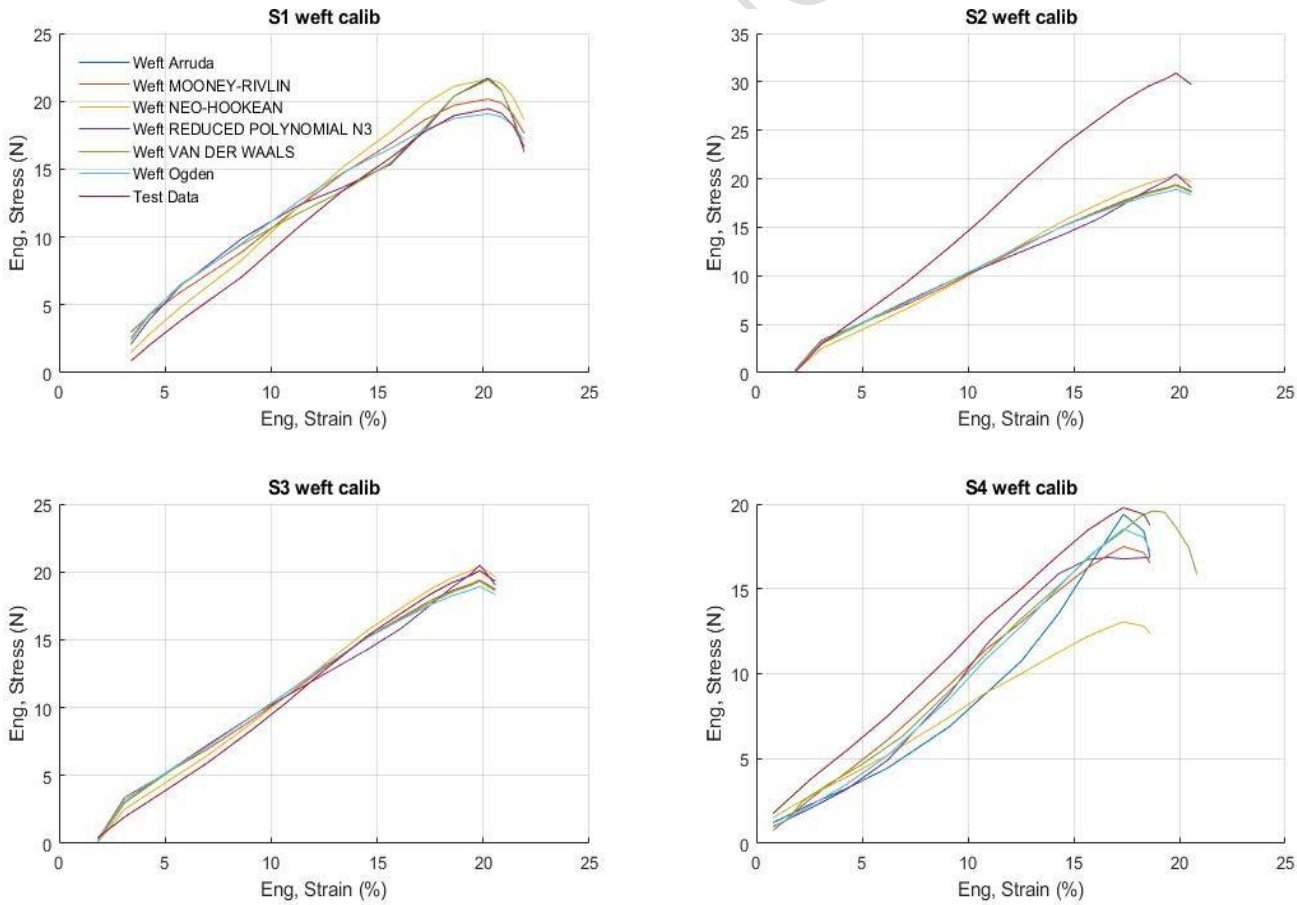

Fig. 6 Fitting hyperelastic models to all sample weft experimental findings

The Mooney-Rivlin model secures the second-highest R-squared value for three samples, thus suggesting that the Mooney-Rivlin model is also a good fit for the experimental data but might outperform the Neo-Hookean model. On the other hand, the Ogden, Arruda-Boyce, and Van-der-Waals models exhibit lower R-squared values and do not align with the data as effectively as the Neo-Hookean or Mooney-Rivlin models.

Analyzing these results is crucial for comprehending the mechanical behavior of the material in various orientations. This comprehension is pivotal for enhancing material design and performance in specific applications. Therefore, conducting material characterization tests under diverse loading conditions is vital to acquiring precise and reliable data. These findings can provide valuable insights into the material's behavior and support the development of new, innovative materials tailored to diverse engineering applications.

Notably, among the tested samples, samples 3 and 4 in each orientation exhibit the lowest error rates during calibration, as depicted in Figures 5 and 6. These observations underscore the suitability of the Neo-Hookean and Yeoh models, particularly the reduced polynomial N3 variant, for effectively characterizing the behavior of the geotextile samples in both the warp and weft directions.

By adhering to specific foundational hypotheses in experimentation, it has been possible to effectively demonstrate the similarity of geotextile samples to the original material and facilitate the calibration of various hyperelastic material models in warp and weft directions. The hyperelastic material models considered in this study encompass the Mooney-Rivlin, Ogden, Arruda-Boyce, Neo-Hookean, Yeoh, and Van-der-Waals models.

The Mooney-Rivlin model calculates strain energy density using the principal strain invariants, while the Ogden model considers three principal stretches. These models have proven invaluable for accurately characterizing the mechanical behavior of the geotextile samples in various orientations.

When modeling hyperelastic materials, it's common to utilize a scalar-valued energy function contingent on the right Cauchy-Green deformation tensor. Nonetheless, invariants or stretches are frequently more convenient for practical implementation in finite element analysis (FEA) codes. This paper presents the successful calibration of material models through Abaqus code test results and numerical simulations.

The behavior of geosynthetics over time, as discussed in reference **(**Luo et al.,2019) is defined by creep and relaxation curves. Consequently, it is essential to account for the influence of time when assessing material performance. One method for modeling time-dependent materials involves employing exponential basis functions within a Prony series. When subjected to prolonged stress, materials enduring continuous stress can undergo cracking and relaxation.

The paper primarily concentrates on applying Finite Element Analysis (FEA) in stretching tests, particularly in the context of hyperelastic models. The paper encompasses a range of facets, including the calibration and simulation of these models within the FEA framework.

5. Stretching Tests Simulation

This section is dedicated to stretching tests conducted using hyperelastic models calibrated through finite element analysis (FEA) (Luo et al.,2019). One of the prominent challenges in FEA simulations involves establishing the shape of the part(s) to be simulated, configuring loading and boundary conditions, and specifying material properties. The examples showcased in this section illustrate that stress calculations obtained from FEA simulations can anticipate material behavior, enhance strength ratios, and streamline the design of intricate components.

Accepted / Not Edited

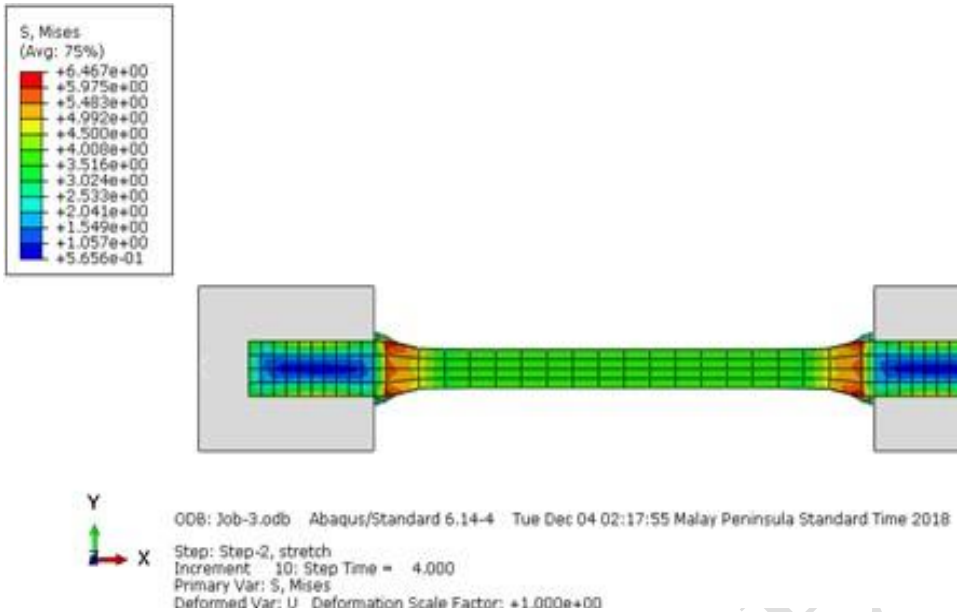

Fig. 7: Abaqus model for weft stretch simulation based on experimental data

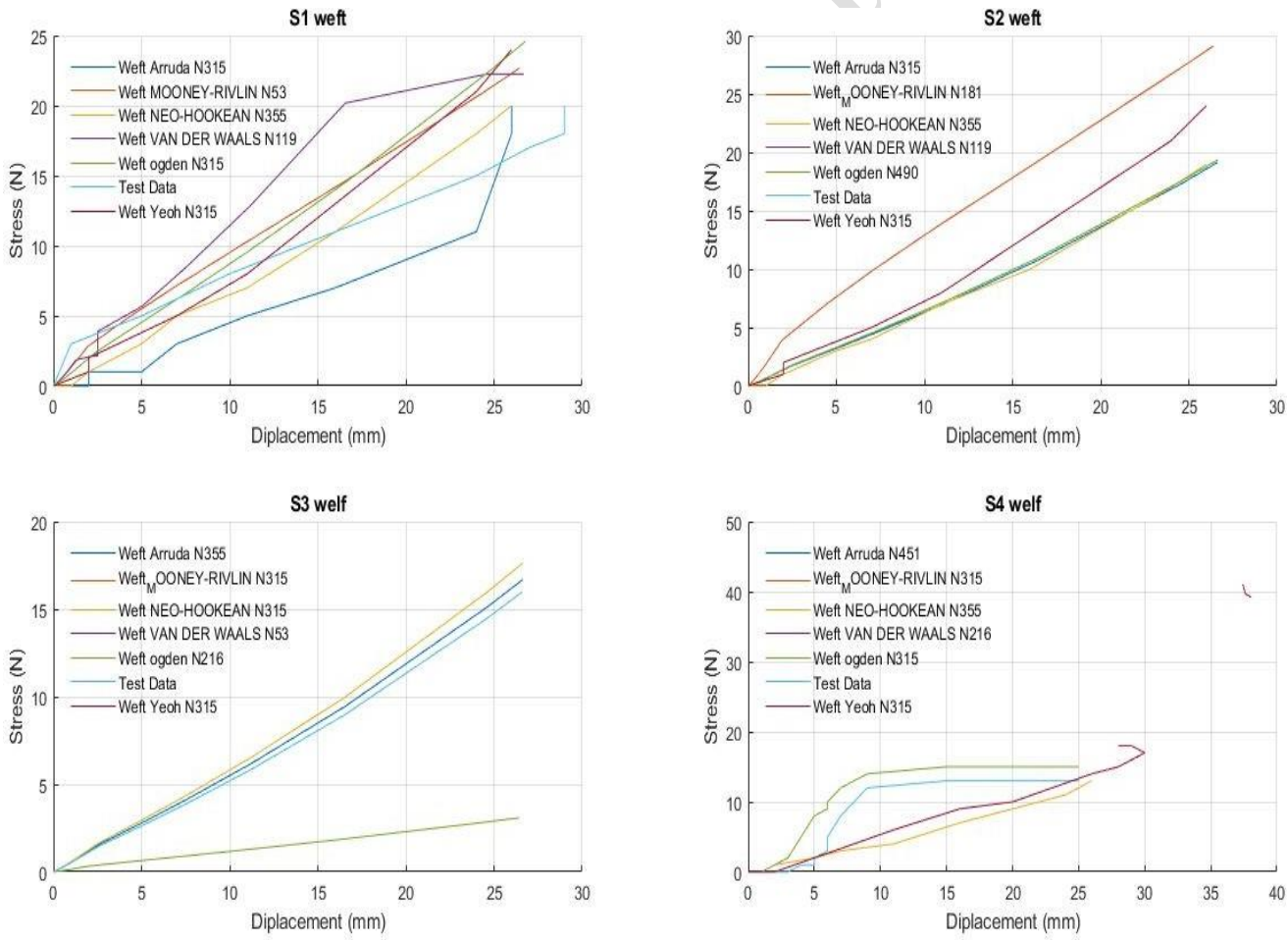

Fig. 8 Examination of FEA predictions (Abaqus): simulation of frame stretching based on experience.

Figure 8 depicts an Abaqus model employed for a weft stretch simulation, utilizing hyperelastic models previously calibrated in Section 3.3. The finite element model in Figure 7 represents a stretching test conducted on a geotextile sample. The hyperelastic material model, tailored for the weft direction, effectively approximates the sample's behavior under the prescribed boundary conditions. One end of the sample experiences a 50 mm enforced displacement in the stretching direction (Ux), while the other is clamped. The model comprises 320 hybrid brick elements (C3D8H) for the sample and two bilinear rigid quadrilateral elements (R3D4) for the clamps. It's worth noting that the gripping step must be iterated 500 times to accurately capture the sample's behavior.

The hyperelastic models, Yeoh and Neo-Hookean, which have been calibrated as outlined in Table 3 and Figure 4, offer a stable and dependable analytical representation of the stress-strain relationship of the material. The numerical results closely align with the experimental data, demonstrating a solid agreement. Nevertheless, it's essential to acknowledge that viscous materials release energy during deformation, and the simulated test samples can influence the material's behavior. Despite this limitation, the uniaxial stress-strain test provides ample insights into the behavior of geotextiles, and modeling can provide valuable information for integrating the material's properties into the design process.

Recognizing that the energy dissipated during material deformation and using simulated test samples can modify the material's behavior is essential. Therefore, while the uniaxial stress-strain test offers valuable insights into the geotextile's behavior, simulation can further enhance the comprehension and utilization of its characteristics in the design process. However, it's essential to acknowledge that simulation results only encompass a portion of the material's behavior, and even minor movements can substantially influence pressure changes owing to quasi-incompressibility. Consequently, care must be exercised when employing simulation outcomes in the design of geotextiles.

6. Conclusion

Calibrating hyperelastic material models is pivotal for thoroughly comprehending how geotextiles react to stress, strain, and energy dissipation during deformation. In this study, the authors harnessed quasi-incompressibility and strain energy as fundamental components to fulfill this objective. Phenomenological models, frequently relying on invariants like polynomials, are extensively utilized in finite element codes for their integration. This research introduces a physically meaningful and mathematically rigorous method, offering a structured approach for selecting suitable geotextile constituent models. challenging to predict in civil engineering applications.

Findings may only be universally applicable to some types of geotextiles. Despite these limitations, this study provides valuable. Moreover, the calibration of hyperelasticity models considers time-dependent behaviors such as creep and relaxation, which are essential for assessing a material's performance under sustained stress conditions. With its contributions, this research facilitates the choice of suitable material models for finite element simulations, ultimately augmenting the precision of geotextile analysis.

It's crucial to recognize that the models developed in this study were specifically customized to match uniaxial tension tests conducted in both the warp and weft directions. However, it's important to note that these insights into geotextile behavior. It lays a foundation for selecting polymers with interface material properties, which can be In our case, the scope of our study is limited to unidirectional testing of geotextiles. That means we are not considering other types of testing, such as biaxial or triaxial.

Our findings may not apply to geotextiles subjected to forces in multiple directions. It is a relatively narrow scope, and we need help to generalize the behavior of geotextiles in other loading conditions. Our findings may not apply to geotextiles subjected to different loading conditions, such as compression, tension, or shear. We acknowledge the significance of extending the relevance of our findings to orientations other than warp and weft. To tackle this aspect, we plan to

Accepted / Not Edited

conduct supplementary experiments and analyses to assess geotextile behavior under diverse loading conditions comprehensively.

7. Nomenclature.

PET:	Polyethylene terephthalate
RMS:	Root Mean Squared Error
FEA:	Finite Element Analysis
SLS:	The Linear Solid Model
W :	Strain Energy Potential
λ_i:	Principal Stretches
μ_i:	Material Constant Related to Shear Modulus
α_i:	Empirically Calculated Material Constant
j_{el} :	Elastic Volume Ratio
N :	Polynomial Order of the Strain Energy Function
C_{ij} :	Material Shear Behavior Constant
D_i:	Constant for Incompressible Materials
Δσe:	Represents the discrete increase in stress during phase I of deformation.
Δσk:	This variable represents the discrete increase in stress during phase II of deformation.
Δεe:	Corresponding to phase I, this variable represents the discrete increase in strain.**δ
TU	The nominal stress
$C10$	The Neo-Hookean material parameter
λ	the stretch ratio

8. Acknowledgement

The author would like to express gratitude to the Laboratory Built Env and the Department of Civil Engineering at USTHB University for their support in completing this work. Special thanks go to the faculty members for their assistance and guidance throughout the project.

9. References

Arruda, E. M., & Boyce, M. C. (1993). “On the dynamic electromechanical loading of dielectric elastomer membranes”. *J. Mech. Phys. Solids*, *41*, 389. DOI: 10.1016/0022-5096(93)90025-5.

Brinson, H. F., & Brinson, L. C. (2008). *Polymer engineering science and viscoelasticity. An introduction*, 99-157.

Barbero, E. J. (2023). *Finite Element Analysis of Composite Materials using Abaqus®*. CRC press.

Chevalier, L., Luo, Y. M., Monteiro, E., & Menary, G. H. (2012). “On visco-elastic modelling of polyethylene terephthalate behaviour during multiaxial elongations slightly over the glass transition temperature”. *Mechanics of Materials*, *52*, 103-116. DOI: 10.1016/j.mechmat.2012.05.003.

Chevalier, L., Marco, Y., & Regnier, G. (2001). "Modification des propriétés durant le soufflage des bouteilles plastiques en PET."*Mécanique & industries*, *2(3)*, 229-248.

Carreau, P. J., De Kee, D. C., & Chhabra, R. P. (2021). *Rheology of polymeric systems: principles and applications*. Carl Hanser Verlag GmbH Co KG.

Gavin, H. P. (2019). "The Levenberg-Marquardt algorithm for nonlinear least squares curve-fitting problems.". *Department of civil and environmental engineering, Duke University*, *19*.

Guo, Z., Fei, J., & Jie, Y. (2022). "An equivalent-additional-stress-based material point method for the deformation of reinforced soil slopes under supergravity." *Computers and Geotechnics*, *142*, 104536. DOI: 10.1016/j.compgeo.2021.104536.

Ding, L., Xiao, C., & Cui, F. (2023). "Analytical model for predicting time-dependent lateral deformation of geosynthetics-reinforced soil walls with modular block facing.” *Journal of Rock Mechanics and Geotechnical Engineering*.

Heymans, N. (2004). "Fractional calculus description of non-linear viscoelastic behaviour of polymers." *Nonlinear dynamics*, *38*, 221-231.DOI: 10.1007/s11071-004-3757-5.

Hackett, R. M. (2016). *Hyperelasticity primer*. Cham: Springer International Publishing.

Hieu, Dang Minh, et al. (2023). "Study on Tensile Strength of High-Density Polyethylene/Polyethylene Terephthalate Blend." *Advances in Machinery, Materials Science and Engineering Application IX*. IOS Press, 27-32.

IsO, E. N. "10319. (2008) Geosynthetics–Wide-width tensile test." *International Organization for Standardization, Geneva, Switzerland*.

Jeon, H., An, B., Kim, H., Kim, Y., Cui, G., & Jang, Y. (2008). “Stress relaxation behaviors of nonwoven geotextile composites.” *Geosynthetics in Civil and Environmental Engineering*, pp. 20–24. DOI: 10.1007/978-3-540-69313-05.

Kang, M. J., Kim, B. S., Hwang, S., & Yoo, H. H. (2018). ”Experimentally derived viscoelastic properties of human skin and muscle in vitro”. *Medical Engineering & Physics*, *61*, 25-31.

Kenja, K., Madireddy, S., Vemaganti, K. (2020)."Calibration of hyperelastic constitutive models: the role of boundary conditions, search algorithms, and experimental variability." *Biomechanics and Modeling in Mechanobiology*

Accepted / N

19(5), 1935–1952. DOI: 10.1007/s10237-020-01318-3.

Lim, J., Hong, J., Chen, W. W., & Weerasooriya, T. (2011). "Mechanical response of pig skin under dynamic tensile loading". *International Journal of Impact Engineering*, *38*(2-3), 130-135. DOI: 10.1016/j.ijimpeng.2010.09.003.

Li, Y., Tang, S., Kröger, M., & Liu, W. K. (2016). "Molecular simulation guided constitutive modeling on finite strain viscoelasticity of elastomers". *Journal of the Mechanics and Physics of Solids*, *88*, 204-226. DOI: 10.1016/j.jmps.2015.12.007.

Łagan, S. D., & Liber-Kneć, A. (2017). "Experimental testing and constitutive modeling of the mechanical properties of the swine skin tissue". *Acta of bioengineering and biomechanics*, *19*(2), 93-102.

Luo, R. K. (2019). "A general hyperelastic-time model for numerical prediction on rubber relaxation and experimental validation under different environments". *Polymer Engineering & Science*, *59*(10), 2159-2168. DOI: 10.1002/pen.25218.

Mooney, M. (1940). "A theory of large elastic deformation". *Journal of applied physics*, *11*(9), 582-592.

Mansouri, M. R., & Darijani, H. (2014). "Constitutive modeling of isotropic hyperelastic materials in an exponential framework using a self-contained approach". *International Journal of Solids and Structures*, *51*(25-26), 4316-4326. DOI: 10.1016/j.ijsolstr.2014.08.018.

Mihai, L. A., & Goriely, A. (2017). "How to characterize a nonlinear elastic material? A review on nonlinear constitutive parameters in isotropic finite elasticity". *Proceedings of the Royal Society A: Mathematical, Physical and Engineering Sciences*, *473*(2207), 20170607.

Mokhireva, K. A., & Svistkov, A. L. (2020). "A new approach to describe the elastic behavior of filled rubber-like materials under complex uniaxial loading". *International Journal of Solids and Structures*, *202*, 816-821.

Narayanan, P., Pramanik, R., & Arockiarajan, A. (2023). "A hyperelastic viscoplastic damage model for large deformation mechanics of rate-dependent soft materials". *European Journal of Mechanics-A/Solids*, *98*, 104874.

Peng, F. L., Li, F. L., Tan, Y., & Kongkitkul, W. (2010). "Effects of loading rate on viscoplastic properties of polymer geosynthetics and its constitutive modeling". *Polymer Engineering & Science*, *50*(3), 550-560.

Powell, P. C., & Housz, A. I. (2023). *Engineering with polymers*. CRC Press.

Rivlin, R. (1948). Large elastic deformations of isotropic materials. I. "Fundamental concepts." *Philosophical Transactions of the Royal Society of London. Series A, Mathematical and Physical Sciences*, *240*(822), 459-490.

Sawicki, A., Kazimierowicz-Frankowska, K. (1998). "Creep behavior of geosynthetics." *Geotextiles and Geomembranes 16(6)*, 365–382. DOI: 10.1016/S0266-1144(98)00020-X.

Shahzad, M., Kamran, A., Siddiqui, M.Z., Farhan, M. (2015). "Mechanical characterization and FE modeling of a hyperelastic material." *Materials Research 18*, 918–924. DOI: 10.1590/1516-1439.320414.

Saberi, E., Najar, S. S., Abdellahi, S. B., & Soltanzadeh, Z. (2017). "A hyperelastic approach for finite element modelling puncture resistance of needle punched nonwoven geotextiles". *Fibers and Polymers*, *18*, 1623-1628. DOI: 10.1680/gein.14.00023.

Treloar, L. (1943). "The elasticity of a network of long-chain molecules—ii." *Transactions of the Faraday Society 39*, 241–246.

Treloar, L.G. (1975). *The physics of rubber elasticity*. OUP Oxford.

Treloar, L., Riding, G. (1979). "A non-Gaussian theory for rubber in biaxial strain: mechanical properties." Proceedings of the Royal Society of London. A. *Mathematical and Physical Sciences 369(1737)*, 261–280. DOI: 10.1098/rspa.1979.0163.

Van Lancker, Bert, Wouter De Corte, and Jan Belis (2020). "Calibration of hyperelastic material models for structural silicone and hybrid polymer adhesives for the application of bonded glass." *Construction and Building Materials* 254: 119204.

Ward, Ian M., and John Sweeney (2012). *Mechanical Properties of Solid Polymers*.John Wiley & Sons.

Wang, J.-Q., Xu, L.-J., Lin, Z.-N., Tang, Y. (2020). "Study on creep characteristics of geogrids considering sand-geosynthetics interaction under different loading levels." *Journal of Engineered Fibers and Fabrics* 15, DOI: 10–117715589250209585.

Wu, H., Yao, C., Li, C., Miao, M., Zhong, Y., Lu, Y., Liu, T. (2020) "Review of application and innovation of geotextiles in geotechnical engineering." *Materials 13(7)*, 1774.

Yun, S., Jung, J., Jun, S., Jeong, J., Moon, Y.H., Kim, J.H. (2021). "Constitutive and fracture modeling of biaxially oriented polyethylene terephthalate film and its application to polymer-coated sheet metal forming." *Journal of Manufacturing Science and Engineering 143(6)*, 061005 .

Zohra, B.F., Fouad, B.A., Mohamed, C. (2022). "Soil-structure interaction interfaces: literature review." *Arabian Journal of Geosciences 15*(12), 1–16. DOI: 10.1007/s12517-022-10336-7.